ELSEVIER

Thin Solid Films 405 (2002) 135–140

thin solid films

www.elsevier.com/locate/tsf

Nanoscale morphology of polyelectrolyte self-assembled films probed by scanning force and near-field scanning optical microscopy

Geoffrey M. Lowman, Steven K. Buratto*

Department of Chemistry and Biochemistry, University of California, Santa Barbara, Santa Barbara, CA 93106-9510, USA

Received 26 January 2001; received in revised form 9 April 2001; accepted 7 September 2001

Abstract

We applied shear force microscopy, an analog to attractive-mode atomic force microscopy, and near-field scanning optical microscopy (NSOM) to the study of surface roughness and nanoscale morphology in polyelectrolyte self-assembled layers. Our data show that the surface roughness of multilayer films on glass grows linearly with the number of polyelectrolyte bilayers for the first 10 bilayers, and then asymptotes at a surface roughness of 4 nm. The surface of these films is characterized by bumps of 100–500 nm in diameter and 25–50 nm tall. In addition, the size and density of the bumps for each bilayer are uncorrelated to the previous surface. This result is in sharp contrast to what is observed for other self-assembled layer structures, such as metal-phosphonate and Langmuir–Blodgett self-assembly, where the surface roughness linearly increases with the number of layers. Subsurface morphology in thin films was observed via fluorescence NSOM of a dye-doped polyelectrolyte film. The NSOM images show domains of higher and lower fluorescence intensity, which could be assigned to local changes in the film thickness, suggesting that the dye molecules are uniformly distributed within the film. We also show that both the initial and asymptotic surface roughness can be dramatically decreased if the bare glass surface is treated with a high charge-density polyelectrolyte, such as poly(ethyleneimine) (PEI), prior to the bilayer formation. Finally, we observed that if the initial substrate is rough, growth of the polyelectrolyte layers acts to smooth the surface until the equilibrium value is reached.

Keywords: Self-assembly; Multilayers; Surface roughness

1. Introduction

Polyelectrolyte self-assembly has shown promise as a route for fabricating thin organic films with controlled thickness and functionality. Polyelectrolyte self-assembly begins with a substrate with an excess surface charge, and alternating layers of polyanions and polycations are deposited on the charged substrate by dipping into a solution of the polyelectrolyte salt. Thin films of a wide variety of functionalities have been demonstrated using this technique, including conducting and semiconducting polymers [1–4], polynucleotides [5], liquid crystals [6], gold nanocrystals [7] and ferroelectric polymers [6]. Light-emitting diodes (LEDs) produced from alternating layers of poly(sodium *p*-styrenesulfonate) (PSS) and poly(*p*-phenylene vinylene) (PPV) fabricated through polyelectrolyte self-assembly have been demonstrated, indicating that electrical contacts, as well as electrical conduction, are possible in these self-assembled films [1,2].

This method has been described as producing 'fuzzy' layers, since the resulting films are, in general, disordered in the plane of the substrate, but are well-ordered in the growth direction and have a well-defined thickness [8–10]. This method has several advantages over Langmuir–Blodgett deposition and self-assembly methods based on co-ordination chemistry. These include: deposition from solution by dipping; extreme flexibility (i.e. no specific functional group is required beyond a positive or negative charge); the absence of large strain between layers; and the ability to 'heal' defects formed in previous layers [11]. Healing of defects formed in previous layers has been shown by several groups and

* Corresponding author. Tel.: +1-805-893-3393; fax: +1-805-893-4120.

E-mail address: buratto@chem.ucsb.edu (S.K. Buratto).

0040-6090/02/$ - see front matter
PII: S0040-6090(01)01669-8

has been explained by the flexible polyelectrolyte layers either filling in voids or smoothing out bumps. The layers are held together through the ionic interaction of the oppositely charged polyelectrolyte. A critical feature of this method is that it is self-limiting [8–10,12]. Once charge reversal of the substrate surface is achieved, growth is stopped due to repulsive interaction between the new surface and the polyelectrolyte with the same charge. The thickness of each layer is, thus, very well defined and remains linear for the deposition of >100 layers, producing films of macroscopic dimensions (100 μm–10 mm) [8–10,12].

Current methods of analysis of polyelectrolyte self-assembled films, including such spatially averaged techniques as ellipsometry, grazing-angle X-ray diffraction, neutron diffraction and UV-Vis spectrophotometry, indicate well-ordered layer-by-layer growth. While these techniques are essential for probing physical properties of the overall film, little is known regarding the mesoscale morphology and its influence on the material properties. The polyelectrolyte requires that the properties defined on a nanoscale in an individual layer extend to the macroscale. We have observed that the relationship between the nanoscale properties and the morphology is critical to a detailed understanding of the properties of the film as a whole.

In this paper, we applied scanned probe microscopy techniques to show that polyelectrolyte films are smooth on the 10-nm scale and that the surface roughness asymptotes after only 10 bilayers. In addition, films prepared with an initial layer of poly(ethyleneimine) (PEI) show smoother surfaces than layers prepared on bare glass. We determined that the surface roughness of fluorescein-labeled polyelectrolyte films is slightly higher than the unlabeled films. We used a combination of both NSOM and shear force microscopy to simultaneously image the fluorescence and topography of the film, respectively. We stress that these images are independent and that for films with no dye, the shear force technique yields a topography image from which we determine the surface roughness. The combination of NSOM and shear force microscopy allows us the ability to compare the topography observed from both optically inactive films and dye-labeled films with the fluorescence observed from optically active films. Using NSOM, we determined that the increased surface roughness leads to fluorescence contrast. The changes in fluorescence intensity as a function of position were attributed to changes in the thickness of the film, indicating that the dye molecules are uniformly distributed on a 100-nm scale. We also show that the polyelectrolyte self-assembly has the ability to smooth rough surfaces, providing direct confirmation of the healing properties on the nanometer scale.

2. Experimental

2.1. Instrumentation

The NSOM/shear force apparatus used for studying polyelectrolyte films has been described in detail elsewhere [13]. Near-field excitation was accomplished using a subwavelength aperture at the end of a tapered optical fiber coated with 100 nm of Ag [14]. The tapered fibers were fabricated using a commercial pipette puller with a 10-W CO_2 laser as the heat source. Metallization of the fiber tips was carried out using thermal evaporation at a base pressure of 2×10^{-6} torr with the tips positioned at a slight angle to shadow the end from the metal source. All of the tips used in our experiments were optimized for throughput of the excitation wavelength, 488 nm from an Ar^+ laser, and yielded a maximum illumination power of 1 kW/cm^2.

The standard, optically detected shear-force technique [15,16], an analog to attractive-mode atomic force microscopy (AFM), was used to maintain the tip within the near-field ($\sim$10 nm) of the surface of the film. This feedback mechanism also provides an independent topography image of the surface by raster scanning the sample while keeping the tip fixed. In images of polyelectrolytes which are not fluorescent, the shear force microscopy was performed with an uncoated fiber to improve the resolution by eliminating the thickness of the metal coating. Rastering of the sample was controlled with commercial scanning-probe microscopy electronics (Digital Instruments, Santa Barbara, CA).

Root mean-squared surface roughness was calculated using the following equation [17]:

$$\mathrm{rms}=\sqrt{\frac{(Z_i-Z_{\mathrm{ave}})^2}{N}} \tag{1}$$

where Z_i refers to the height on the Z-axis of feature i in the topology of the image, Z_{ave} is the average height of the entire image, and N is the number of pixels in the image.

In FL-NSOM, the fluorescence signal is collected with a high numerical aperture (N.A.$=0.85$) objective and routed to either an avalanche photodiode (APD) for imaging or to a spectrometer/CCD detector for spectroscopy via the optics of a conventional optical microscope. The excitation wavelength is suppressed with a holographic notch filter.

2.2. Polyelectrolyte self-assembly

Polyelectrolyte self-assembled films were prepared on microscope cover glass (Fisher, size $25\times25\times0.5$ mm^3) or quartz cover slips (Chemglass Inc, size $19\times19\times0.5$ mm^3). Ultra-purified (Millipore) water (pH 5.5) was used for all preparation steps. Polyelectrolyte multilayers

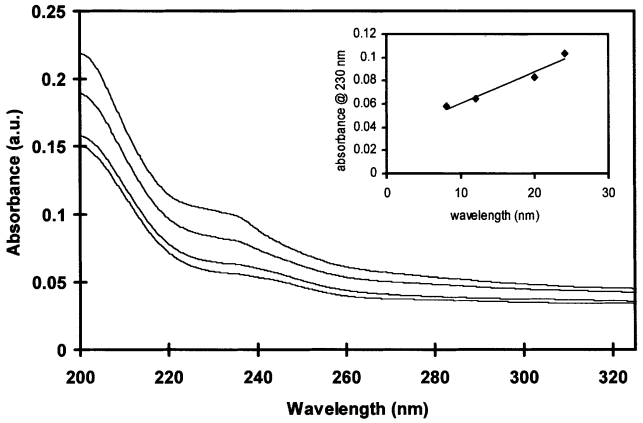

Fig. 1. UV/Vis absorption spectra of an 8-, 12-, 20- and 28-bilayer PAH/PSS thin film. Inset shows the linear relationship between absorption of PSS at 230 nm and the number of bilayers deposited.

were produced via the self-assembly process described by Decher and co-workers [8–10,18]. Poly(sodium *p*-styrenesulfonate) (PSS) was purchased from Acros Organics. Poly(allylamine hydrochloride) (PAH) and fluorescein isothiocyanate (FL) were purchased from Aldrich. Poly(ethyleneimine) (PEI) was purchased from Polysciences Inc. All materials were used without further purification. Glass surfaces were cleaned by immersion in a Piranha solution, H_2SO_4/H_2O_2 (7:3), and sonicated for 1 h and then rinsed with ultra-pure water and dried. This process produces a hydrophilic glass surface with an excess negative charge. Substrates were then sonicated for 1 h in $H_2O/H_2O_2/NH_4OH$ (5:1:1) (RCA) solution, rinsed and dried. Rough glass substrates for the surface smoothing experiment were prepared by etching the coverslip in 15% HF for 2 min.

PAH was covalently labeled with fluorescein using a procedure previously reported [19]. This reaction produced a dye concentration of 1 per 20 monomer units as measured by UV-Vis spectroscopy, consistent with the results reported in [19].

Adsorption of PEI, PAH, and PSS was carried out in 0.02 M aqueous solutions [8–10,12]. Fl-PAH was adsorbed from a 7 mM solution in ethylene glycol, which was made slightly basic by the addition of solid sodium hydroxide. Films were prepared by sequential dipping of the functionalized substrates in the appropriately charged polyelectrolyte solution. Typically, a single layer of PAH or PSS was deposited by immersion for 15–20 min in the polyelectrolyte solution, followed by rinsing with ultra-pure water and drying. Dye-labeled PAH was adsorbed from a 10-min immersion, rinsed with ethanol/ultra-pure water/ethanol, and then dried. Film growth was monitored by UV-Vis spectroscopy and small-angle X-ray diffraction.

3. Results and discussion

An example of a PAH\PSS film growth cycle, studied by UV-Vis spectroscopy (Shimadzu UV-1601), is shown in Fig. 1. UV-Vis spectra from one polyelectrolyte thin-film sample after deposition of 8, 12, 20, and 28 bilayers of PAH\PSS are shown. Film growth was studied by monitoring the absorption of the phenyl chromophore on the PSS polymer chain at approximately 238 nm. It is evident from Fig. 1 that as the number of bilayers deposited is increased, the shoulder in the absorption spectrum at 238 nm is also increased due to the increased amount of PSS present in the film. The inset in Fig. 1 shows the absorbance of the phenyl group on PSS as a

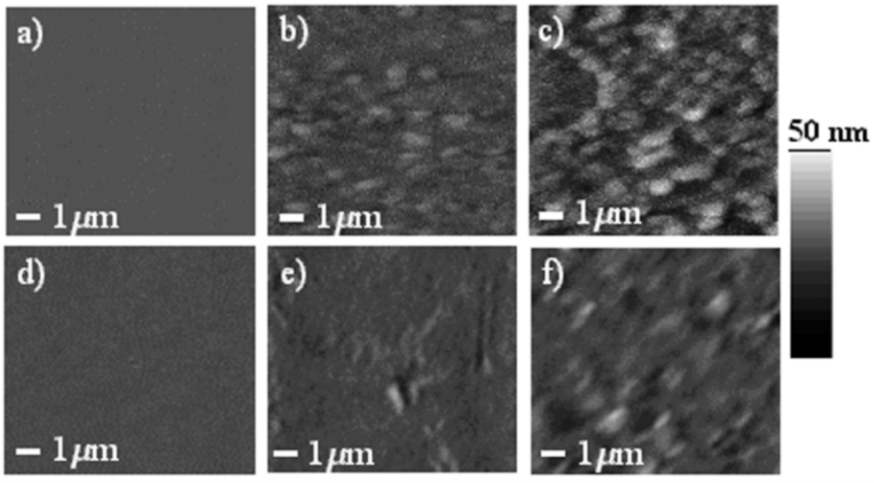

Fig. 2. Comparison of surface topography of thin films of PEI\PSS(PAH\PSS)$_x$ and (PAH\PSS)$_x$. Shear force images of: (a, d) glass substrates cleaned with piranha and RCA solution; (b) a 2-bilayer film of PAH\PSS; (c) a 10-bilayer film of PAH\PSS; (e) a 2-bilayer film of PEI\PSS\(PAH\PSS)$_1$; and (f) a 10-bilayer film of PEI PSS\(PAH\PSS)$_9$. Images have been adjusted to show maximum contrast and the depth of contrast in all images is 40%.

function of the number of bilayers. As can be observed from the graph, the film growth proceeds as a stepwise and linear process [12]. The film thickness as measured by small-angle X-ray diffraction was 2.2 nm per bilayer.

Fig. 2 shows typical shear force topography images taken from thin films of PAH\PSS grown on bare glass (Fig. 2a–c) and on a PEI-treated surface (Fig. 2d–f) after zero, two and 10 bilayers, receptively. Fig. 2a shows an image of a bare glass surface after cleaning with Piranha and RCA solutions, with no visible features present in the image. Upon addition of two bilayers to the bare glass surface, several ($\sim$50) small raised features appear on the surface (Fig. 2b). These features have a diameter of a few 100 nm and a height of approximately 25 nm, consistent with previous studies on a similar system using AFM [20]. After the addition of 10 bilayers (Fig. 2c), the density of these features has increased so that they cover most of the surface, but their size remains approximately the same. Images of films with greater than 10 bilayers (not shown) are very similar to that of Fig. 2c and little change in the surface topography is observed after the deposition of 10 bilayers. A dramatic change in the surface topography is observed if the glass surface is treated with PEI prior to bilayer deposition. Fig. 2d shows the topography of the PEI-treated glass surface and the surface appears featureless and very similar to the bare glass surface of Fig. 2a. After deposition of two bilayers (Fig. 2e), small features appear that are far less numerous than in the film without the PEI layer (Fig. 2b). After deposition of 10 bilayers (Fig. 2f), the density of the small features has increased, but this density and the size of the features is smaller than in the 10-bilayer film grown on bare glass (Fig. 2c).

It is possible to gain further insight into the surface morphology by monitoring the increase in surface roughness as a function of the number of layers. As discussed in the previous section, the rms roughness is a measure of the fluctuations in the height of the surface. If the surface topography is characterized by features with similar dimensions, then the rms roughness is related to the density of these features. Fig. 3 shows the rms roughness of both the polyelectrolyte film grown on bare glass (■) and the film grown on the PEI-treated glass (▲). As expected from the topography images, there are distinct differences in the two curves. The film deposited on bare glass shows surface roughness values ranging from approximately 2.0 nm for the first layer deposited, steadily increasing to 3.8 nm after five bilayers, and again reaching a constant value of approximately 3.9 nm after 10 bilayers have been deposited. The film deposited on PEI-treated glass, however, shows much lower surface roughness. For this film, the surface roughness values range from approximately 1.2 nm for the primary layer containing PEI, slowly rising with added PAH\PSS bilayers to approximately 1.7 nm,

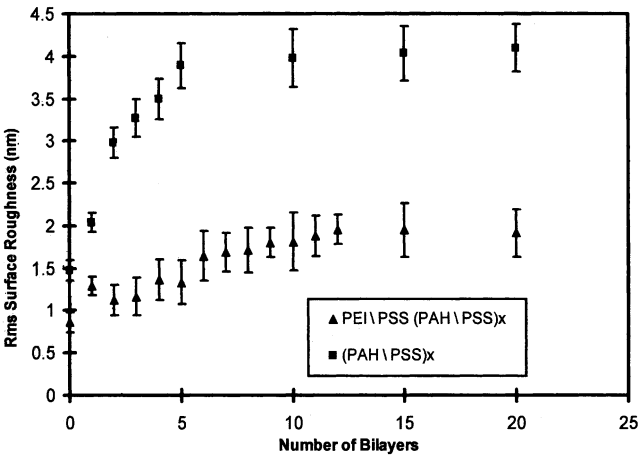

Fig. 3. Root mean-square surface roughness values calculated from shear force measurements during assembly of two different polyelectrolyte films. The plot shows the difference in surface roughness between a film containing PEI\PSS(PAH\PSS)$_x$ (▲) and a film containing only (PAH\PSS)$_x$ (■). Surface roughness measurements for each growth step were made by calculating the RMS roughness at 10 different places on the film using the commercial scanning electronics. The error bar shown for each point is the standard deviation from the average roughness at each film growth step measured.

where they also appear to plateau after the deposition of 10 bilayers.

There are several important points that can be drawn from the data of Figs. 2 and 3. Since both the morphology observed and the surface roughness of the polyelectrolyte films grown on bare and PEI-treated glass reach a steady-state value, these surface features are most likely related to the intrinsic morphology of the polyelectrolyte layers rather than to nucleated defects. This is in stark contrast to films fabricated by Langmuir–Blodgett or metal phosphonate self-assembly, where the number of surface features and the surface roughness linearly increase with the number of layers and the size of surface bumps increases with the number of layers. The steady-state value of the surface roughness is dependent on the initial charge density of the substrate. In the case of a bare glass surface, the charge density is low and the resulting roughness is higher than if the charge density of the substrate is high, as is the case for the PEI-treated glass. This result is consistent with the previous conclusion that using a primary layer of PEI, a highly branched polyelectrolyte, improves film adhesion and lowers the interface roughness as further layers are deposited [21–24]. These results imply that the deposition of polyelectrolyte layers has the ability to ‘smooth-out’ or ‘heal’ a rough surface, since the steady-state surface topography is dependent on the intrinsic morphology of the polyelectrolytes and not on the topography of the substrate. The ‘healing’ nature of polyelectrolyte layers has previously been postulated by several groups [8,11].

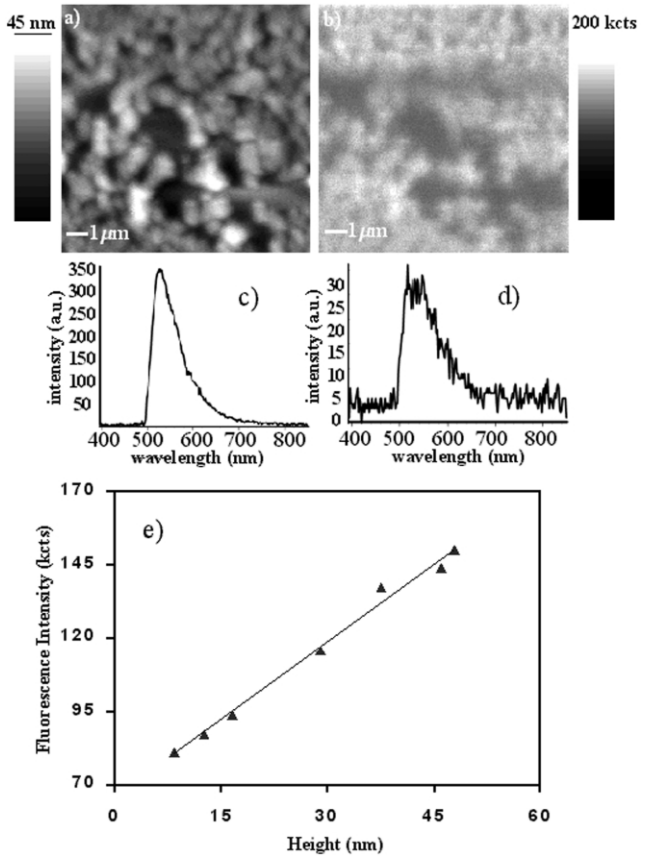

Fig. 4. (a) Shear force topography and (b) NSOM images of a 9-bilayer film of FL-PAH\PSS. Correlation is shown between raised features in the topography image and bright features in the NSOM fluorescence image, and conversely, between low points in the topography and dim features in the NSOM image. Images have been adjusted to show maximum contrast. Depth of contrast in the shear force image is 95% and 50% for the NSOM image. Spatially localized fluorescence spectra of the FL-PAH taken from bright (c) and dim (d) regions in image (b) are also shown. (e) Linear relationship between feature height and fluorescence intensity for seven spots in the fluorescence image.

Films containing bilayers of FL-PAH\PSS were studied using fluorescence NSOM in order to probe the interior morphology. A two-fold increase in surface roughness is observed in FL-PAH\PSS films when compared to PAH\PSS films deposited on glass substrates that were previously studied. Fig. 4 shows both (a) shear force topography and (b) NSOM fluorescence images taken simultaneously of a nine-bilayer film of FL-PAH\PSS. There is a one-to-one correlation between the raised features in the topography image and bright features in the NSOM fluorescence image, and between low points in the topography image and dim features in the NSOM fluorescence image. By comparing the change in height from the low to the high spots in Fig. 4a and the change in fluorescence intensity from the dark to the bright spots in Fig. 4b, the contrast observed can be completely attributed to changes in the film thickness. Fig. 4e shows the feature height and fluorescence intensity of seven points in the images in Fig. 4a,b. The resulting linear relationship between feature height and fluorescence intensity implies that although contrast is observed in the FL-NSOM image (Fig. 4b), the fluorescein molecules are uniformly dispersed throughout the film and no phase separation is observed on the 100-nm scale. In addition, the NSOM technique also provides the ability to carry out spatially localized fluorescence spectroscopy, as shown in Fig. 4c,d. These spectra were collected from bright and dim spots in the NSOM image as indicated in (b); both spectra were collected with 10-s integration times. We note that the fluorescence spectra differ only in their intensity and that the fluorescence lineshapes are identical. This is further indication that no phase separation of the dye molecules is observed, which would result in concentration quenching, aggregate emission and a broader lineshape [25].

Finally, the capability of a self-assembled PE thin film to heal a rough surface was examined by starting the deposition on a rough glass surface. Fig. 5 shows shear force topography images taken from (a) a glass surface that has been intentionally roughened by etching

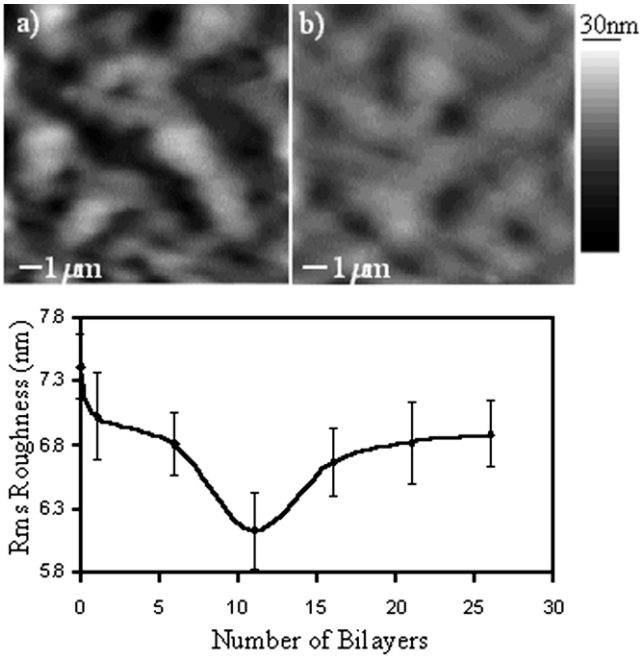

Fig. 5. Surface smoothing capability of polyelectrolyte multilayers. Shear force topography images taken from (a) a glass surface that has been intentionally roughened, and (b) the same glass surface after growth of 11 bilayers of PAH\PSS. Both images are shown with equal contrast and height scale to show smoothing of the rough surface. A plot of the root mean-square surface roughness values calculated from shear force measurements of a PAH\PSS film that was assembled on a glass surface that had been intentionally roughened is shown in (c). A marked decrease in surface roughness is shown for up to 11 bilayers of film deposited.

in a solution in 15% HF in ethanol, and (b) the same glass surface after growth of 11 bilayers of PAH\PSS. The roughened glass surface shows very pronounced crevices relative to image (b), and results in an rms roughness value of 7.4 nm. After deposition of six bilayers of PAH\PSS, this value dropped to 6.8 nm, and after 11 bilayers the roughness was further reduced to 6.1 nm. The image of the surface after deposition of 11 bilayers shows a significant reduction in the surface topography features over that of the rough glass substrate. Clearly, the surface has been 'healed' by the deposition of polyelectrolyte bilayers, resulting in a smoother surface with fewer defects. It is curious to note that after further deposition cycles, the rms roughness reaches an equilibrium roughness of approximately 6.7 nm. While this is still lower than the initial 7.4-nm surface roughness of the etched glass, there appears to be a memory of the rough surface.

4. Conclusions

We have shown that a combination of scanning force and near-field scanning optical microscopy can yield important insight into the nanoscale morphology of polyelectrolyte self-assembled layers. Our results show that the surface topography is characterized by bumps of 100–500 nm in diameter and 25–50 nm tall. The density of these features reaches a steady-state value after deposition of 10 bilayers. Films prepared with an initial layer of poly(ethyleneimine) (PEI) show smoother surfaces than layers prepared on bare glass, indicating that the steady-state density of features is dependent on the charge density of the surface. We also showed that the polyelectrolyte self-assembly technique has the ability to smooth rough surfaces, providing direct confirmation of the healing properties on the nanometer scale. Finally, we showed that the surface roughness of fluorescein-labeled polyelectrolyte films is slightly higher than the unlabeled films and that the fluorescein dye is uniformly distributed throughout the film.

Acknowledgments

This work was supported by the David and Lucille Packard Foundation, the NSF Nanotechnology Initiative and the Alfred P. Sloan Foundation.

References

[1] A.C. Fou, O. Onitsuka, M. Ferreira, M.F. Rubner, B.R. Hsieh, J. Appl. Phys. 79 (1996) 7501.
[2] O. Onitsuka, A.C. Fou, M. Ferreira, B.R. Hsieh, M.F. Rubner, J. Appl. Phys. 80 (1996) 4067.
[3] J.H. Cheung, W.B. Stockton, M.F. Rubner, Macromolecules 30 (1997) 2712.
[4] W.B. Stockton, M.F. Rubner, Macromolecules 30 (1997) 2717.
[5] G.B. Sukhorukov, H. Mohwald, G. Decher, Y.M. Lvov, Thin Solid Films 285 (1996) 220.
[6] J. Reibel, M. Brehmer, R. Zentel, G. Decher, Adv. Mater. 7 (1995) 849.
[7] J. Schmitt, G. Decher, W.J. Dressick, et al., Adv. Mater. 9 (1997) 61.
[8] G. Decher, Science 277 (1997) 1232.
[9] H. Mohwald, Colloids Surf. A: Physiochem. Eng. Aspects 171 (2000) 25.
[10] P.T. Hammond, Curr. Opin. Colloid Interface Sci. 4 (2000) 430.
[11] E.R. Kleinfeld, G.S. Ferguson, Chem. Mater. 8 (1996) 1575.
[12] J.D. Hong, J. Schmitt, G. Decher, Thin Solid Films 210/211 (1992) 831.
[13] K.D. Weston, J.A. DeAro, S.K. Buratto, Rev. Sci. Instrum. 67 (1996) 2924.
[14] E. Betzig, J.K. Trautman, T.D. Harris, J.S. Weiner, R.L. Kostelak, Science 251 (1991) 1468.
[15] E. Betzig, P.L. Finn, J.S. Weiner, Appl. Phys. Lett. 60 (1992) 2484.
[16] R. Toledo-Crow, P.C. Yang, Y. Chen, M. Vaeziravani, Appl. Phys. Lett. 60 (1992) 2957.
[17] Digital Instruments, Command Reference Manual, version 4.10.01, Santa Barbara, CA, 1995 [www.digitalinstruments.com].
[18] J.D. Hong, G. Decher, Macromol. Chem. Macromol. Symp. 46 (1991) 321.
[19] D.M. Kaschak, T.E. Mallouk, J. Am. Chem. Soc. 118 (1996) 4222.
[20] G.J. Kellogg, A.M. Mayes, W.B. Stockton, M. Ferreira, M.F. Rubner, S.K. Satija, Langmuir 12 (1996) 5109.
[21] K. Ariga, Y. Lvov, T. Kunitake, J. Am. Chem. Soc. 119 (1997) 2224.
[22] A.C. Fou, O. Onitsuka, M. Ferreira, M.F. Rubner, B.R. Hsieh, J. Appl. Phys. 79 (1996) 7501.
[23] R.V. Klitzing, H. Mohwald, Thin Solid Films 284/285 (1996) 352.
[24] C. Tedeschi, F. Caruso, H. Mohwald, S. Kirstein, J. Am. Chem. Soc. 122 (2000) 5841.
[25] N.J. Turro, Modern Molecular Photochemistry, University Science Books, Sausalito, CA, 1991.